ORIGINAL ARTICLE

Bone-derived MSCs encapsulated in alginate hydrogel prevent collagen-induced arthritis in mice through the activation of adenosine $A_{2A/2B}$ receptors in tolerogenic dendritic cells

Gaona Shi[a], Yu Zhou[a], Wenshuai Liu[b], Chengjuan Chen[a], Yazi Wei[a], Xinlong Yan[c], Lei Wu[a], Weiwei Wang[b,*], Lan Sun[a,*], Tiantai Zhang[a,*]

[a]*State Key Laboratory of Bioactive Substance and Function of Natural Medicines, Institute of Materia Medica, Chinese Academy of Medical Sciences & Peking Union Medical College, Beijing 100050, China*
[b]*Tianjin Key Laboratory of Biomaterial Research, Institute of Biomedical Engineering, Chinese Academy of Medical Sciences & Peking Union Medical College, Tianjin 300192, China*
[c]*Faculty of Environmental and Life Sciences, Beijing University of Technology, Beijing 100124, China*

Abstract Tolerogenic dendritic cells (tolDCs) facilitate the suppression of autoimmune responses by differentiating regulatory T cells (Treg). The dysfunction of immunotolerance results in the development of autoimmune diseases, such as rheumatoid arthritis (RA). As multipotent progenitor cells, mesenchymal stem cells (MSCs), can regulate dendritic cells (DCs) to restore their immunosuppressive function and prevent disease development. However, the underlying mechanisms of MSCs in regulating DCs still need to be better defined. Simultaneously, the delivery system for MSCs also influences their function. Herein, MSCs are encapsulated in alginate hydrogel to improve cell survival and retention *in situ*, maximizing efficacy *in vivo*. The three-dimensional co-culture of encapsulated MSCs with DCs demonstrates that MSCs can inhibit the maturation of DCs and the secretion of pro-inflammatory cytokines. In the collagen-induced arthritis (CIA) mice model, alginate hydrogel encapsulated MSCs induce a significantly higher expression of $CD39^+CD73^+$ on MSCs. These enzymes hydrolyze ATP to adenosine and activate $A_{2A/2B}$ receptors on immature DCs, further promoting the phenotypic transformation of DCs to tolDCs and regulating naïve T cells to Tregs. Therefore, encapsulated MSCs obviously alleviate the inflammatory response and prevent CIA progression. This finding clarifies the mechanism of MSCs-DCs crosstalk in

eliciting the immunosuppression effect and provides insights into hydrogel-promoted stem cell therapy for autoimmune diseases.

1. Introduction

Rheumatoid arthritis (RA) is a chronic autoimmune and inflammatory disorder marked by the infiltration of immune cells into joint synovial compartments and the generation of persistent immune responses against self-antigens. This causes bone and cartilage destruction, functional impairment, and eventual disability[1−4]. Currently, three classes of drugs including glucocorticoids (GCs), disease-modifying antirheumatic drugs (DMARDs), and nonsteroidal anti-inflammatory drugs (NSAIDs), are prescribed for RA to alleviate the symptoms. However, these drugs have limitations as they often require high doses to achieve satisfactory results, which results in unwanted side-effects[5,6]. Although kinase inhibitors and biological agents can provide substantial anti-arthritic effects by suppressing immune cells, there is an increased risk of infection and tumorigenicity[7]. Despite the significant progress in drug development against autoimmune diseases in the past decade, a substantial percentage of patients still experience chronic inflammation and progressive disability[8,9]. Hence, there is an urgent need for novel strategies on restoring self-tolerance by amending dysregulated immune responses to effective treat autoimmune disorders.

The dysfunction of immune tolerance is critical in the pathogenesis of autoimmune diseases, such as RA. Therefore, restoring immune tolerance is a realistic strategy for the treatment of RA. MSCs, being multipotent progenitor cells, have the ability to regulate the maturation of DCs, the differentiation of T and B cells, and the polarization of macrophages[10]. Recent studies have shown that MSCs can mitigate the symptoms of autoimmune arthritis and other inflammatory diseases[11,12], but certain issues need to be clarified for MSCs to treat RA. Firstly, the crosstalk of MSCs in the local joint and adjacent cells depends on their number, retention, and viability in situ[13,14]. Biomaterials can provide support for MSCs and the surrounding cells. Encapsulation of MSCs in three-dimensional (3D) scaffolds such as hydrogels can improve their retention, viability, immunomodulatory properties, and therapeutic efficacy in vivo[15,16]. Hydrogels synthesized from alginate are highly suitable for biomedical applications due to their low toxicity, low cost, good gelling capacity, and high bioavailability[17]. Ionically cross-linked injectable alginate hydrogel is an ideal cell delivery scaffold for tissue regeneration[18]. Secondly, the exact mechanism of MSCs in restoring the immune tolerance of DCs remains to be further elaborated. It is reported that pro-inflammatory cytokines such as interferon-γ (IFN-γ) can enhance the immunosuppressive function of MSCs. The expression of CD39 and CD73 on MSCs can promote adenosine production, which participates in the interactions of MSCs and other cells. Nonetheless, the ability of MSCs to directly promote tolerogenic dendritic cells (tolDCs) in vivo in an inflammatory microenvironment, as well as the underlying mechanisms and therapeutic potential, remains unclear.

In this work, we hypothesize that ionically cross-linked injectable alginate hydrogel is an ideal scaffold for delivering MSCs. Alginate hydrogel can improve the viability, retention, and proliferation of MSCs in vivo, and it can also enhance their immunomodulatory effect towards endogenous DCs. Based on the encapsulation of MSCs in alginate hydrogel 3D scaffolds, we aim to investigate the underlying mechanism of MSCs on DCs in CIA. Our results suggest that encapsulation of MSCs in alginate hydrogel induces tolDCs and Treg cells through the CD39/CD73/adenosine axis to ameliorate inflammation and autoimmunity, affecting the arthritis progression mediated by mature DCs after recognizing autoantigen. This finding provides insight into novel therapeutic strategies for autoimmune diseases.

2. Materials and methods

2.1. Agents, antibody, and cytokines

Alginate (CAS: 9005-38-3) was purchased from Meilunbio (Dalian, China). All anti-mouse antibodies including CD86-PE (#105008), CD11c-APC (#117310), I-A/I-E-PercP Cyanine 5.5 (#107626), CD73-APC (#127210), CD39-PE (#143804), Ly-6A/E (Sca-1)-FITC (#108105), CD44-PE (#103007), CD45-FITC (#103108), PDL1-PE Cy7 (#124314), and CD11b-FITC (#101206) were procured from Biolegend (San Diego, CA, USA). Calcein AM and propidium iodide (PI) were purchased from Immunochemistry (Lumington, CA, USA). Recombinant murine IL-4 (#214-14) and GM-CSF (#315-03) were obtained from PeproTech (Rocky Hill, NJ, USA), LPS-EB (CAS: 5969-42-02), and lipopolysaccharide from *Escherichia coli 0111: B4* strain was purchased from Invivo Gen (Hong Kong, China). The selective adenosine A_{2A} receptor (A_{2A}R) antagonist SCH58261 (HY-19533) and the selective adenosine A_{2B} receptor (A_{2B}R) antagonist LAS01057 (HY-14390) were purchased from MedChemExpress (Shanghai, China). The DiR cell membrane fluorescent probe (MB12482, Meilunbio) was procured from Meilunbio. The Toxin Sensor™ Chromogenic LAL Endotoxin Assay Kit (GenScript, Piscataway, NJ, USA) was used to exclude endotoxin contamination during hydrogel preparation. The endotoxin level in the alginate hydrogel was lower than 0.1 endotoxin unit/mL.

2.2. Mice

The 6−8-week-old female DBA/1 mice, 2-week-old female C57BL/6 mice, and 6-8-week-old female C57BL/6 mice were purchased from Huafukang Co., Ltd. (Beijing, China) and housed in a pathogen-free facility under controlled humidity, temperature, and a 12-h light/dark cycle. They were fed with a standard diet with freely available food and sterile water. All animal experiments were approved by the Animal Care and Use Committee of the Institute of Materia Medica, Chinese Academy of Medical

Sciences & Peking Union Medical College (Approval No. 00005368). Animals were acclimatized for at least one week before the experiments. All cell lines were tested and confirmed to be free of Mycoplasma and other rodent pathogens by the China Centre for Type Culture Collection (CCTCC). No other authentication assay was performed.

2.3. Preparation and characterization of MSCs loaded alginate hydrogel

To prepare hydrogel, the alginate polymer was dissolved in α-MEM solution and the percentages of 1.0%, 2.5%, and 5.0% (w/v) were used. Then 2% (w/v) $CaCl_2$ solution was added into each alginate solution (volume ratio for 1% alginate: $CaCl_2$ = 10 : 1, 2.5% alginate: $CaCl_2$ = 10 : 1, 5% alginate: $CaCl_2$ = 10 : 1). Alginate hydrogel was formed after stirring for a few minutes (2 min). The gelation was measured via test tube inversion. The rheological analysis of 5.0% alginate hydrogel or 5.0% alginate hydrogel encapsulated MSCs was performed by AR 2000ex rheometer (TA) according to a previously reported method[19]. The modulus change was recorded at a fixed angular frequency of 1 rad/s and shear strain of 1%, respectively. The internal morphology of the hydrogel was observed by scanning electron microscopy (Phenom Pro, Phenom-World, Eindhoven, the Netherlands). Briefly, the alginate hydrogel was quick-frozen in liquid nitrogen and lyophilized, and at least three random areas were photographed for the morphology of the hydrogel.

2.4. Cell culture and imaging

DBA/1 or C57BL/6 mice bone-derived MSCs were isolated and cultured according to the protocol previously reported[20]. A 2-week-old mouse was sacrificed by cervical dislocation and rinsed in 75% (v/v) ethanol for 2 min. Then the mouse was placed in a 100-mm sterile dish and the hindlimbs were incised from the trunk. Muscles and tendons were cleaned from femurs and tibiae using dissecting scissors. The bones were placed on a sterile dish and the attached soft tissue was removed from the bone. A syringe needle was inserted into the bone cavity and marrow was flushed out with α-MEM medium to deplete hematopoietic cells. Then, the chips were suspended approximately 1-3 mm^3 in 5 mL of α-MEM containing 10% fetal bovine serum (FBS) in the presence of 1 mg/mL collagenase II. The chips were digested for 2 h in a shaking incubator with a shaking speed of 200 rpm at 37 °C. The collagenase digestion was stopped, and the digestion medium was discarded. The bone chips were washed with 5 mL of α-MEM three times. And the chips were seeded into a 100 mm dish in the presence of 10 mL α-MEM containing 10% FBS. Incubated in a 5% CO_2 incubator at 37 °C and cultured for three days. On Day 3, the medium was changed, and 10 mL of α-MEM supplemented with 10% FBS was replaced. On Day 5, the adherent cells were harvested by digesting with 0.25% trypsin. The cells at passages 3-8 were used for in vitro and in vivo experiments.

At passage 5, the cells alone or cultured with alginate hydrogel were harvested by trypsinization. The cells were washed and resuspended 1×10^6 cells in 100 μL of cold PBS per EP tube and stained with FITC-conjugated anti-mouse CD11b, CD45 and Ly-6A/E (Sca-1); PE-conjugated anti-mouse CD86, CD39, and CD44; PercP Cyanine 5.5-conjugated anti-mouse MHCII, APC-conjugated anti-mouse CD73. The cells were analyzed by flow cytometry analysis, and data were analyzed by FlowJo7.6 software.

DCs were generated from bone marrow cells as previously described[21,22]. Bone marrow cells were flushed out of the mice's femur and tibia in PBS and centrifuged. The single cells were resuspended in RPMI 1640 supplemented with 10% FBS, and 100 mg/mL penicillin/streptomycin) containing 20 ng/mL recombinant murine GM-CSF (315-03, PeproTech) and 10 ng/mL recombinant murine IL-4 (#214-14, PeproTech) at a density of 5×10^6 cells/mL and dispensed in a 24-well plate. The medium was exchanged on Day 3 to remove the free-floating cells, and fresh medium containing the suitable reagents was added on Day 5. The BMDCs were harvested on Day 7 and stained with anti-mouse PE Cyanine 7-CD11c, PE-CD86, or PercP Cyanine 5.5-MHC II (Biolegend) for phenotypic analysis.

2.5. MSCs viability assay in 3D alginate hydrogel

The harvested MSCs (passage 4, 5×10^5 cells/mL) were suspended in 1.0%, 2.5%, and 5.0% alginate hydrogel with a volume of 0.1 mL, and the MSCs/alginate hydrogel mixtures were incubated in 24-well culture plates for 48 h. After 48 h of spheroid embedding, live/dead assay was performed for examination of cell viability. MSCs encapsulated in each concentration of alginate hydrogel were incubated in Calcein AM solution 1:500 (C3099, v/v) for 5 min and 1: 200 (v/v) of PI in the medium at standard culture condition (5% CO_2 at 37 °C) for 10 min. After washing with PBS, the 3D MSCs sphere was observed under a fluorescence microscope (Cytation 5, BioTek, Winooski, CA, USA).

Bone marrow-derived dendritic cells (BMDCs) (2×10^5 cell/well) were incubated with or without the presence of E. coli O111:B4 LPS (100 ng/mL), alginate hydrogel, or MSCs (1×10^6 cell/well), at 37 °C for the indicated time.

2.6. Measurement of cytokines production and anti-CII antibody

Cytokines were determined using mouse TNF-α ELISA kit (88-7324-88, Invitrogen, Carlsbad, CA, USA), mouse IL-6 ELISA kit (#88-7064-88, Invitrogen), mouse IL-10 ELISA kit (#88-7105-88, Invitrogen), mouse IL-12p70 ELISA kit (#88-7121-88, Invitrogen), mouse IFN-γ ELISA kit (#88-7314-88, Invitrogen), mouse IL-17A ELISA kit (#88-7371-88, Invitrogen) following the manufacture's protocols. The supernatant from cells in different treatment groups (LPS-stimulated BMDCs were used as model group, BMDCs, LPS stimulated BMDCs together with alginate hydrogel, LPS-stimulated BMDCs co-cultured with MSCs were used as control groups, for the group of MSCs co-culture BMDCs group, MSCs were seeded at the density of 5×10^5 cell/mL to 24-well plate 24 h before co-cultured with BMDCs, for the reverse validation experiment, the $A_{2A/2B}R$ inhibitors together with LPS stimulated BMDCs co-cultured with MSCs encapsulated alginate hydrogel were also used, encapsulated MSCs in alginate hydrogel was prepared 24 h before co-cultured with BMDCs) as added to ELISA plate coated with capture antibody and incubated at room temperature for 2 h. After washing 3 times, the detection antibody was added to each well and incubated at room temperature for 2 h. After washing 3 times, Avidin-HRP was added and incubated at room temperature for 30 min. TMB solution was added to each well after washing 5 times. The plate was read at 450 nm after adding the stop solution. Cytokines concentration was calculated in each treatment sample using the standard curve.

The levels of TNF-α, IFN-γ and IL-10 in the serum of CIA mice were also measured with ELISA kits. In addition, serum levels of anti-CII antibodies were detected using an established

ELISA. The wells of a 96-well plate were coated with 500 ng of CII collagen and incubated at 4 °C overnight, then washed 3 times with PBST. The serum samples were obtained on Day 42 after treatment and diluted to 10,000 times. The diluted serum samples were added to the plate, then incubated at 37 °C for 1 h. After washing the plate 3 times with PBST, total anti-CII antibody levels were detected with HRP-conjugated goat anti-mouse IgG (Southern Biotech, Birmingham, AL, USA).

2.7. In vivo cell survival and proliferation assay

Mouse bone-derived MSCs were cultured in α-MEM medium, trypsinized, and labeled with 1 μmol/L DiR at 37 °C for 20 min. $5 \times$ volume of 10% FBS was added and centrifuged at 1200 rpm for 5 min and repeated 3 times. Then, 1×10^6 MSCs labeled with DiR were re-suspended in 100 μL PBS, or alginate hydrogel scaffold. 100 μL blank alginate hydrogel was injected as the control group. Cells were transplanted at the right abdomen of the mouse. Mice were anesthetized by isoflurane and imaged on Days 1, 2, 3, 5, 7, and 14 after subcutaneous (s.c.) injection using IVIS SPECTRUM CT equipment with a cooled charge-coupled device camera (Caliper Life Sciences, Hopkinton, MA, USA). The exposure time was 1−2 min and average fluorescence intensity was recorded. Regions of interest were drawn over the transplantation site with the highest signal in each group. All data were analyzed using living image software (V4.2, Caliper Life Sciences).

2.8. Immune response assessment

The histology and flow cytometry analysis were performed to assess the immune response. Histology-encapsulated MSCs were subcutaneously transplanted at the abdomen of 6-8-week-old female C57BL/6 mice ($n = 6$). A group of mice was injected with 100 μL of PBS ($n = 6$) as the control. One week after transplantation, mice were sacrificed, and skin samples and lymph nodes were retrieved. Tissue samples were fixed with 4% paraformaldehyde solution overnight. Sections were stained with hematoxylin and eosin (H&E). Meanwhile, sections were stained overnight with antibody against Ki67 (ab15580, Abcam, Cambridge, UK) at 4 °C, and then was performed using anti-rabbit secondary antibody.

2.9. Induction of collagen-induced arthritis (CIA) mice model and treatment

The induction of arthritis was prepared following a previously described protocol[23]. DBA/1 susceptible mice were immunized by intradermal injection of 100 μL of chicken type II collagen dissolved in 0.05 mol/L acetic acid (4 mg/mL) emulsified in an equal volume of complete Freund's adjuvant (Chendrex, WA, USA) at the tail base. Mice were boosted with chicken type II collagen again on Day 21. According to our preliminary animal experiment and literature[24], a dose of 1×10^6 MSCs per mouse was used in the animal experiment. For the prophylactic treatment regime, on Day 14, mice were randomly divided and received s.c. injection of 1×10^6 MSCs (100 μL), 100 μL of alginate hydrogel, and 1×10^6 MSCs loaded in 100 μL of alginate hydrogel, respectively. Normal and CIA mice were synchronously administrated with equal volumes of PBS. All treatments were performed only once. For the therapeutic regime, on Day 22, mice were randomly divided and received s.c. injection of 1×10^6 MSCs (100 μL), 100 μL of alginate hydrogel, and 1×10^6 MSCs loaded in 100 μL of alginate

hydrogel, respectively. Normal and CIA mice were synchronously administrated with equal volumes of PBS. All treatments were performed only once.

2.10. Clinical assessment of arthritis

Body weight was detected every 2 days from Day 0 to Day 42. For the therapeutic experiment, body weight was detected every 2 days from day 0 to day 56. On Day 22, the clinical score was evaluated every 2 days and the development of arthritis was monitored. The score was generated based on erythema and swelling, and the degree of swelling or loss of function present in each paw was 0−4[25]. The scores of four paws were summed to a total arthritis severity score, giving a maximum score of 16 per mouse. 0 represents no evidence of erythema and swelling; 1 represents erythema and mild swelling confined to the tarsals or ankle; 2 represents erythema and mild swelling extending from the ankle to the tarsals; 3 represents erythema and moderate swelling extending from the ankle to metatarsal joints; 4 represents erythema and severe swelling encompassing the ankle, foot, and digits, or ankyloses of the limb. Paw thickness was measured with a dial-caliper. The hind limbs were photographed and imaged via the Quantum FX imaging system (PerkinElmer, MA, USA) and images were analyzed by Carestream MI SE software. For histological analysis, mice were sacrificed, and the hind limbs were removed, and fixed in 4% paraformaldehyde solution. A 5-μm section was stained with hematoxylin and eosin (H&E) or Safranin O. Histopathological characteristics were examined by microscopy (magnification of $\times$ 100). Synovial proliferation, cellular infiltration, pannus formation, cartilage erosion and inflammation were scored in a blinded manner on a severity scale ranging from 1 to 3 (0: absent; 1: weak; 2: moderate; and 3: severe)[26].

2.11. Ex vivo analysis of antigen presenting cells and Treg cells

Inguinal lymph nodes from CIA mice in different groups were harvested and prepared into single cells suspension. For analysis of cell surface markers, lymphoid cells were directly stained by PE-CD86 (clone: GL-1), PercP Cyanine 5.5-MHCII (clone: M5/114.15.2), and CD73-APC (clone: TY/11.8) antibodies after washed by PBS for 3 times following manufacturer's instructions.

For analysis of intracellular staining, cells were fixed and permeabilized using the Foxp3/transcription factor staining kit (#00-5523-00, eBioscience, San Diego, NY, USA). Samples were measured using flow cytometry BD Verse and data were analyzed by FlowJo software 7.6.

2.12. Verification of signaling pathways

2.12.1. ELISA for measurement of adenosine concentration
ELISA plate was rested at room temperature for 20 min 50 μL of recombinant adenosine standards, supernatant, or serum samples were added to the wells. 100 μL of HRP labeled detection antibody was added to the wells. The plate was incubated at 37 °C for 60 min. Subsequently, the plate was washed 5 times with washing buffer. 50 μL of substrate A and substrate B were added to each well. The plate was incubated at 37 °C for 15 min and avoided light. The reaction was stopped by transferring 50 μL of the stop solution. The absorbance was detected at 450 nm on Synergy H1 microplate reader, BioTek. The adenosine concentration in the samples was determined from a standard curve.

2.12.2. Quantitative real-time PCR

MSCs were prepared as described above, and total RNA was extracted using RNA kit according to the manufacturer's instructions (RNA-Quick Purification Kit, Esunbio, Shanghai, China), cDNA was synthesized using RT-Master Mix (Hifair II 1st Strand cDNA Synthesis Kit, YEASEN Biotech, Shanghai, China). The cDNA product was amplified by quantitative reverse transcription polymerase chain reaction (qRT-PCR) using qTOWER[3] G (Analytikjena AG, Jena, Thuringia, Germany) with relevant primers for mouse. Data were analyzed using the relative gene expression method and were normalized with GAPDH levels in the sample. The measurement of each sample was performed in triplicate. For real-time PCR, the following primers were synthesized by BGI, Tech (Supporting information Table S1).

RT-PCR was performed using qTOWER3 (Analytikjena AG) real-time PCR detection system and the supplied software. A melt curve was performed at the end of each run to ensure a single amplification product. All samples were normalized to the amount of GAPDH mRNA present in each sample. The fold changes in a given gene of interest were determined using the $\Delta\Delta C_T$ method[27].

2.12.3. Intracellular cAMP assay

To determine whether alginate hydrogel loaded MSCs can promote DC cells cAMP secretion, the DC cells co-cultured with MSCs and alginate hydrogel loaded MSCs were collected from different wells post 24 h of co-culture, 0.5 m mol/L IBMX (MCE, HY-12318) was supplemented to the culture media simultaneously. cAMP concentration was measured with cAMP Gs Dynamic kit, and HTRF detection assay kits (62AM4PEB, Cisbio, Bedford, MA, USA) according to the manufacturer's instruction. Briefly, 5 μL of cells (2×10^3) were distributed into each well and 5 μL lysis assay buffer (for the negative control well) or cAMP-d2 working solution (for all other well) was added, and then 5 μL of Anti-cAMP-Cryptate working solution was added to each well. The plate was read on a HTRF-compatible reader (Synergy H1, BioTek) after incubating at room temperature for I h.

2.12.4. Western blotting

After 24 h of co-culture, we transferred the culture media containing the floating MSC 3D spheres in alginate hydrogel from the 24-well plate. The remaining DC cells were then harvested by centrifugation at 3000 rpm for 5 min (SORVALL ST16R Centrifuge, Thermo Scientific, NY, USA), and the supernatant was discarded. The cells were lysed in RIPA buffer. Protein concentration was qualified using the BCA kit. Subsequently, 10 μg of protein was loaded into 10% SDS-polyacrylamide gel electrophoresis for detection of adenosine $A_{2A}R$ (ab3461, Abcam), $A_{2B}R$ (bs-5900R, Bioss-antibodies, Beijing, China), IDO (#68572S, Cell Signaling Technology, MA, USA), phospho-NF-κB P65 (#3033, Cell Signaling Technology), NF-κB P65 (#8242, Cell Signaling Technology) and β-actin (TA-09, ZSGB-BIO, Beijing, China). After incubating with the appropriate HRP-coupled secondary antibodies (ZSGB-BIO), visualization of the protein bands was performed by incubating with Tanon™ Femto-sig ECL Chemiluminescent Substrate (Tanon, Beijing, China) and then documented using the ChemiDoc™ MP system (Tanon).

Isolation of primary T cell and co-cultured with encapsulated MSCs treated DCs *in vitro*: Primary mouse T cells were obtained from draining lymph nodes and mesenteric lymph nodes of C57BL/6 mouse. T cells were initially seeded at 1×10^6 cells in the starting culture system. BMDCs were first pulsed with MSC, alginate hydrogel loaded MSCs, or alginate hydrogel negative control and stimulated alone or with LPS (100 ng/mL) for 24 h and then washed for 3 times. The collected DCs were seeded in 24-well plate at a density of 5×10^5 cells/mL. DCs in each treatment group were cultured either alone or with T cells, at a ratio of 1: 2 (DCs: T cells) in a 24-well plate for 5 days. After 5 days, supernatants were collected for cytokines assay by ELISA kit, IFN-γ and TNF-α for Th1 differentiation, IL-17A for Th17 differentiation and IL-10 for Treg cells assay.

2.13. Statistical analysis

All statistical analyses were performed using GraphPad Prism version 8 (GraphPad, Inc., La Jolla, CA, USA). All data were expressed as mean ± SD for *in vitro* experiments and mean ± SEM for *in vivo* experiments. One-way ANOVA was used to analyze the statistical differences for more than two groups with one factor or two-way analysis of variance (ANOVA), followed by Tukey's post hoc multiple comparison tests. Values of $P < 0.05$ were considered statistically significant.

3. Results

3.1. Synthesis and characterization of bone-derived MSC-loaded alginate hydrogel

Alginate hydrogel (Fig. 1A) utilizing a 5.0% alginate aqueous solution and a 2% CaCl$_2$ aqueous solution (*w/v*) was successfully prepared as previously reported[28]. Iconic bridges among the alginate were formed as the guluronic acid (G unit) blocks interacted with divalent cations (Ca^{2+}), resulting in hydrogel formation. As demonstrated in Fig. 1B, the hydrogel exhibited a porous network structure with a pore size of several microns. Results from the rheological analysis confirmed a significantly higher storage modulus (G') relative to the loss modulus (G") for hydrogel construction (Fig. 1C). Moreover, the modulus of alginate hydrogel, as a function of time was not significantly impacted by the MSC encapsulation (Fig. 1D).

To isolate MSCs, bone fragments were digested using collagenase II as previously described[20]. Within 72 h culture period, fibroblastic colonies were observed and an adherent layer of vortex-shaped fibroblast-like cells was formed within 5 days. The cells had a viability rate of >95% and expressed the mesenchymal marker CD44, as well as stem cell marker Sca-1. Furthermore, CD73 and CD39 were found to be highly expressed in these cells, while the expression levels of CD45, CD11b, and the co-stimulatory molecules CD86 and MHCII were extremely low (Fig. 1E–H). These data demonstrate the successful preparation of MSCs.

The biochemical and mechanical cues of the extracellular matrix (ECM) are critical for the survival, proliferation, and differentiation of MSCs[29]. Therefore, the biomaterial used for encapsulating MSC spheroids should simulate the local microenvironment to optimize the therapeutic effects of MSCs *in vivo*. To this end, we cultured MSCs in alginate hydrogel with different polymer concentrations and analyzed the viability of the embedded cells (Fig. 1I). The MSCs formed 3D spheroids of favorable size when cultured for 48 h in 5.0%, 2.5% and 1.0% (*w/v*) alginate hydrogel, and the percentage of viable cells was 98.89 ± 0.60%, 94.26 ± 1.35%, and 93.16 ± 3.10%, respectively, which was similar to the viability rate of was 96.82 ± 1.30% observed in Matrigel (Fig. 1J). The MSCs cultured in 5.0% alginate hydrogel formed the largest spheroids measuring 264.4 ± 50.8 μm for 24 h, 319.4 ± 41.6 μm for 48 h, and 348.8 ± 83.7 μm for 72 h in diameter (Supporting Information
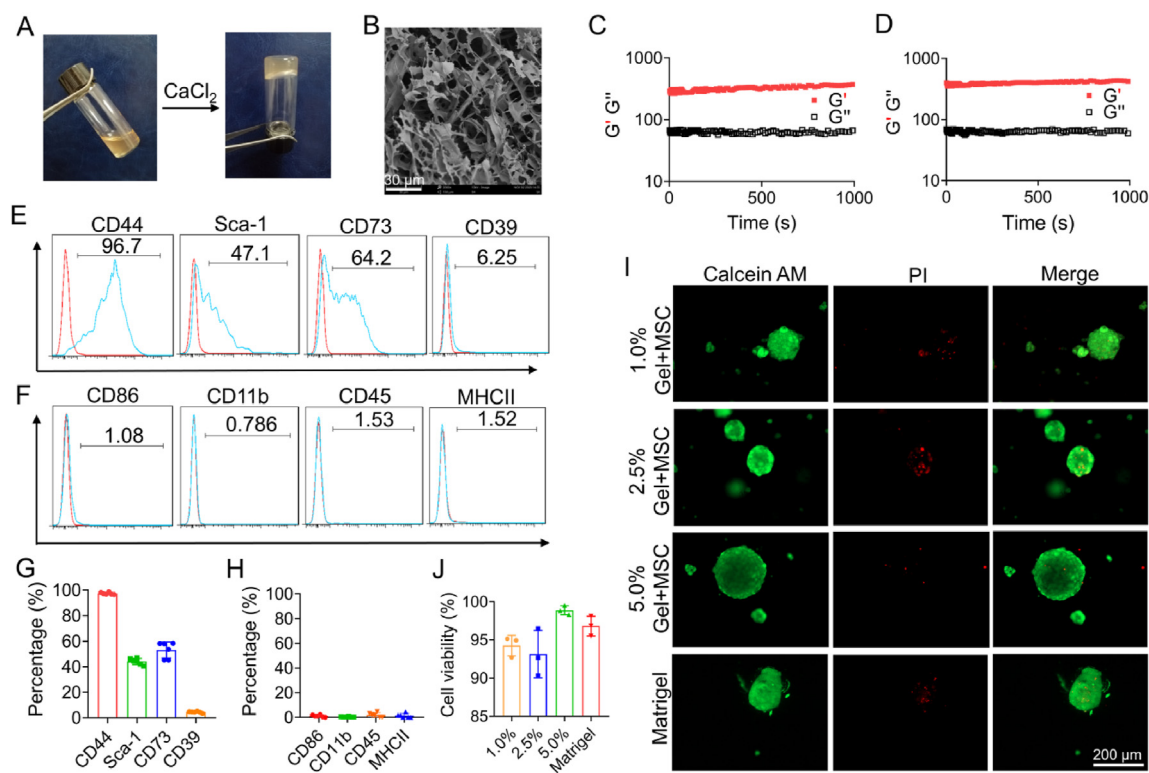
Figure 1   Synthesis and characterization of bone-derived MSC encapsulated alginate hydrogel. (A) Formation of alginate hydrogel. (B) Representative scanning electron microscopy image of lyophilized alginate hydrogel (scale bars = 30 μm). Rheological analysis of alginate hydrogel (C) or MSCs encapsulated alginate hydrogel (D) as a function of time. (E) Expression of mesenchymal marker: CD44, progenitor cells markers: Sca-1, adenosine associated markers: CD73 and CD39. (F) Expression of hematopoietic markers: co-stimulating molecules CD86, CD11b, CD45, and MHCII on mouse bone-derived MSCs. Red lines represent the histogram of negative cells, blue lines represent the histogram of positive cells. (G) Percentages of CD44, Sca-1, CD73, and CD39 on mouse bone-derived MSCs. (H) Percentages of CD86, CD11b, CD45, and MHCII on mouse bone-derived MSCs. (I) Representative fluorescence images for Live/Dead staining. Mouse bone derived MSCs spheroids were formed after culturing in alginate hydrogel for 48 h. All spheroids were generated with an initial number of 12,000 cells/mL. The green and red channels represent the Calcein-AM and PI staining of live and dead cells, respectively. Scale bar = 200 μm. (J) Cell viability of MSCs in different treatment groups. Data are represented as mean ± SD, n = 3.

Fig. S1). Based on these results, 5.0% alginate hydrogel was used for 3D spheroid culturing of MSCs for the subsequent experiments.

3.2.   Encapsulated MSCs inhibit the maturation of bone marrow-derived DCs and prevent the secretion of inflammatory cytokines in vitro

MSCs can disrupt the differentiation of monocytes into DCs, and inhibit the latter's maturation and function, such as the secretion of co-stimulatory molecules and antigen presentation[30]. Furthermore, MSCs can induce the transition of DCs to regulatory DCs, which promotes T-cell anergy and Tregs differentiation. Therefore, we evaluated the effect of the encapsulated MSCs on the maturation and biological activities of DCs. Immature DCs (iDCs) were obtained after culturing bone marrow cells for 5 days in the presence of GM-CSF (20 ng/mL) and IL-4 (10 ng/mL). The LPS-stimulated DCs produced large amounts of the inflammatory cytokines TNF-α (Fig. 2A), and IFN-γ (Fig. 2B). In contrast, the levels of IL-10 in the culture supernatant were low (Fig. 2C). However, DCs co-cultured with encapsulated MSCs produced low levels of TNF-α and IFN-γ, but released high levels of IL-10, an anti-inflammatory cytokine plays a significant role in preventing inflammatory and autoimmune pathologies[31,32].

The iDCs were then co-cultured with bare MSCs, encapsulated MSCs or the empty alginate hydrogel for 48 h in the differentiation medium. Compared to the control group, the encapsulated MSCs can significantly downregulate the co-stimulatory molecules CD86$^+$CD11c$^+$ (Fig. 2D and E) and MHCII$^+$CD11c$^+$ (Fig. 2F and G) and increase the percentage of both CD39$^+$CD11c$^+$ (Fig. 2H and I) and CD73$^+$CD11c$^+$ (Fig. 2J and K). Compared to the control group, the bare MSCs group can increase the expression of CD39$^+$CD11c$^+$ (Fig. 2H and I) and CD73$^+$CD11c$^+$ (Fig. 2J and K) on DCs. Meanwhile, the alginate hydrogel can decrease the expression of CD86$^+$CD11c$^+$ (Fig. 2D and E), MHCII$^+$CD11c$^+$ (Fig. 2F and G), and CD39$^+$CD11c$^+$ (Fig. 2H and I). To better elaborate the effect of encapsulated MSCs on DCs in vitro, we also measured the single positive percentages of CD11c, CD86, MHCII, CD39, and CD73 (Supporting Information Fig. S2). These results indicated that the anti-inflammatory effect and immunoregulatory function of MSCs were enhanced after encapsulating in alginate hydrogel.

3.3.   Encapsulated MSCs in alginate hydrogel increase their survival, proliferation, and immunosuppressive function in vivo

To assess the fate and viability of encapsulated MSCs in vivo, we labeled the MSCs with membrane-specific lipophilic dye DiR and
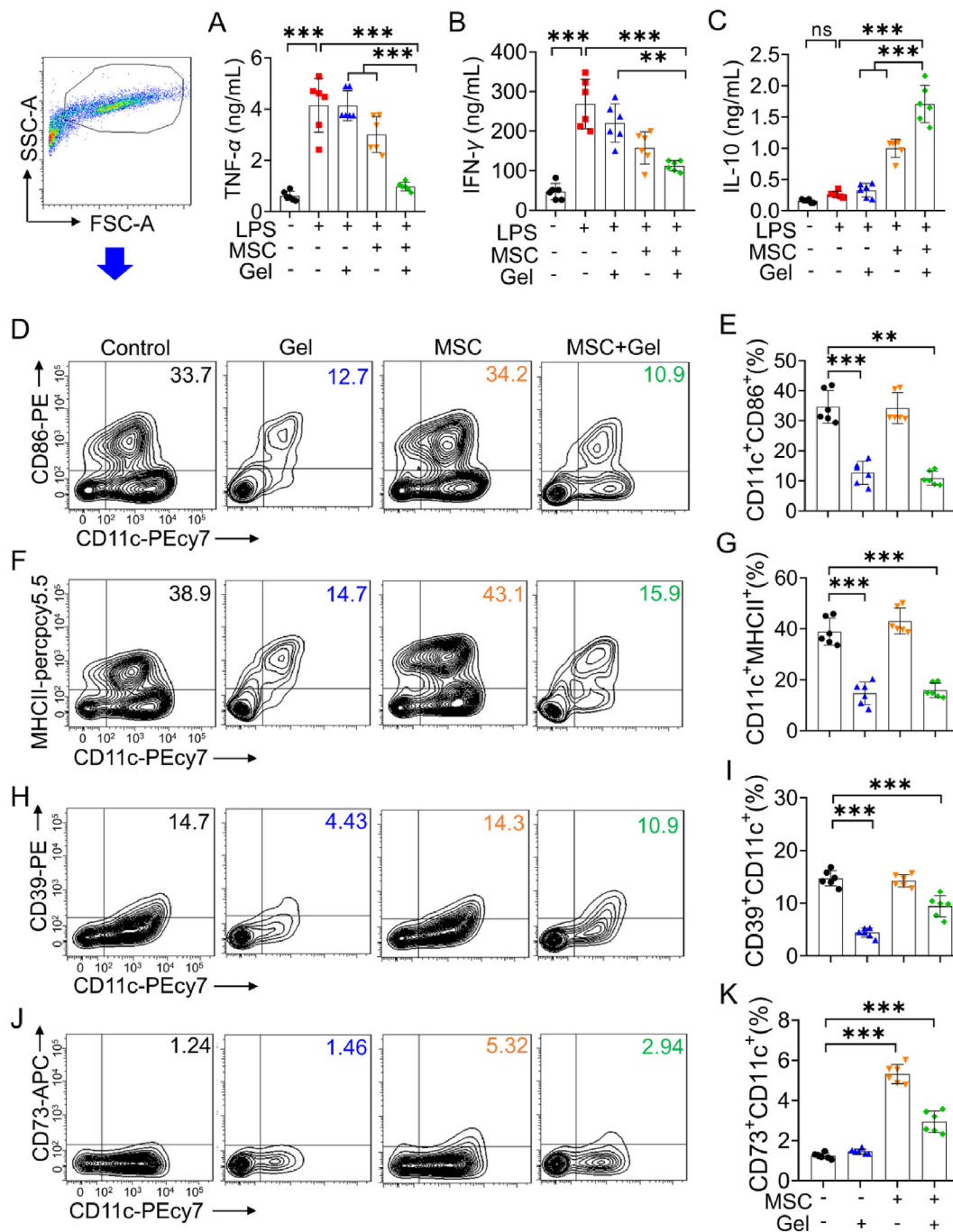
Figure 2 The immunoregulatory effect of encapsulated MSCs on bone marrow-derived DCs *in vitro*. (A) Inhibition of inflammatory mediator TNF-α in LPS-stimulated BMDCs treated with encapsulated MSCs. (B) Expression of inflammatory mediator IFN-γ in LPS-stimulated BMDCs treated with encapsulated MSCs. (C) Promotion of anti-inflammatory mediator IL-10 in LPS-stimulated BMDCs treated with encapsulated. TNF-α, IFN-γ, and IL-10 were measured by ELISA. Flow cytometry analysis and the percentage of CD86$^+$CD11c$^+$ (D, E), MHCII$^+$CD11c$^+$ (F, G), CD39$^+$CD11c$^+$ (H, I), CD73$^+$CD11c$^+$ (J, K) cells in DCs after various treatments. Data are represented as mean $\pm$ SD, $n = 3$; **$P < 0.01$, ***$P < 0.001$ *vs.* indicated.

tracked the bio-distribution of the bare (MSC) and encapsulated MSCs (MSC + Gel) in mice. The mice were subcutaneously transplanted with the same numbers (1×10^6) of MSCs in both groups, or sterile alginate hydrogel as the negative control, and imaged on Days 0, 1, 2, 3, 5, 7, and 14 post-inoculations using IVIS system (Fig. 3A). One day after transplantation, strong fluorescence signals were detected in MSC + Gel group,

suggesting that alginate hydrogel can retain the MSCs at the site of injection. Furthermore, the fluorescence intensity in this group increased significantly over days 2, 3, and 7, suggesting cell survival of MSCs encapsulated in alginate hydrogel. On the other hand, the fluorescence signals of the bare MSCs gradually decayed after the first day post-transplantation, suggesting a lower cell survival rate (Fig. 3B). Very few cells were detected at the
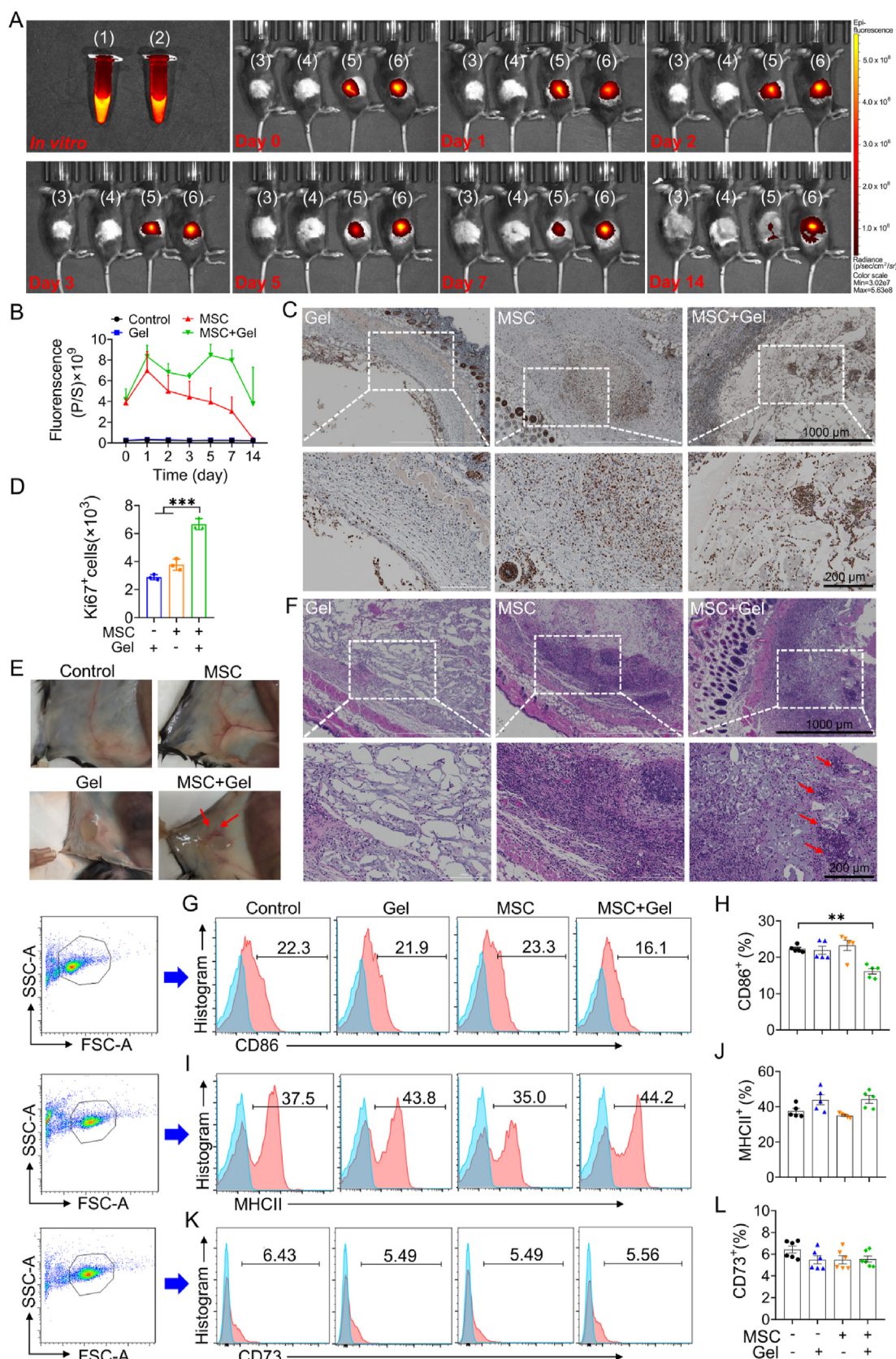
Figure 3 *In vivo* survival, proliferation and immunoregulatory effects of MSCs encapsulated in alginate hydrogel. (A) Viability of MSCs encapsulated in the alginate hydrogel *in vivo*. Representative IVIS images harvested at different time points following s.c. administration of DiR-labeled MSCs imbedded in alginate hydrogel or alone into mice. (1) is the DiR-labeled MSCs *in vitro*, (2) is the DiR-labeled MSCs imbedded in alginate hydrogel *in vitro*, (3) is the mice in the control group, (4) is the mice in alginate hydrogel injection group, (5) is the mice in DiR-labeled

injection site in the MSCs group after 14 days, whereas the resident MSCs in MSC + Gel group at this time point were comparable in number to that on Day 0. Then, the survival and proliferation effect of encapsulated MSCs was further examined through Ki67 immunostaining. Mice from each group were sacrificed on Day 7, and tissue surrounding the scaffold along with MSCs was retrieved and processed for Ki67 immunostaining (Fig. 3C). The counts of Ki67^{+} cells in each treatment group were analyzed using ImageJ software. As shown in Fig. 3D, the number of proliferating Ki67^{+} cells was significantly higher in the MSC + Gel group than in the bare MSC or alginate hydrogel groups. Furthermore, representative photograph and H&E staining of the MSCs-loaded hydrogel and surrounding subcutaneous tissues demonstrated that the implantation of MSCs significantly induced the migration and infiltration of inflammatory immune cells in the vicinity of draining lymph nodes, compared to the injection of hydrogel alone (Fig. 3E and F). Simultaneously, we evaluated the immunoregulatory function of the encapsulated MSCs in normal mice after s.c. injection for 7 days. The phenotype of DCs in the draining lymph nodes was analyzed using flow cytometry. As shown in Fig. 3G—L, the percentage of CD86^{+} DCs decreased significantly ($P < 0.01$) in the MSC + Gel group compared to the hydrogel group (Fig. 3G and H), but no significant difference was observed in the expression of MHCII (Fig. 3I and J) and CD73 (Fig. 3K and L). These results suggested that encapsulated MSCs can decrease the expression of CD86 on resident DCs in normal mice. Meanwhile, the hematological parameters were measured to quantitatively evaluate the safety of encapsulated MSCs *in vivo*. As shown in H&E staining, encapsulated MSCs in healthy mice did not affect tissue structure, or cellular morphology (Supporting Information Fig. S3A). For routine blood examination, the parameters, such as lymphocytes, monocytes, neutrophils, platelet (PLT), hematocrit (HCT), hemoglobin, red blood cells (RBC), white blood cells (WBC), were at a normal level (Fig. S3B). Taken together, encapsulated MSCs in alginate hydrogel exhibited good biocompatibility in mice. Moreover, the survival, proliferation, and immunosuppressive function of MSCs were also improved *in vivo*.

3.4. Encapsulated MSCs dramatically inhibit disease development and inflammatory responses in collagen-induced arthritis (CIA) in DBA/1 mice

CIA model was constructed in DBA/1 mice to further examine the prophylactic effect of the hydrogel encapsulated MSCs (from DBA/1 mice) on the development of arthritis (Fig. 4A). DBA/1 mice were immunized with Collagen/Complete Freund's adjuvant (CII/CFA) emulsion and treated with bare or encapsulated MSCs on Day 14 after the first immunization. As shown in Fig. 4B, the average body weight in MSC + Gel group was enhanced significantly compared to the mice in the model group ($P < 0.001$). There were no significant differences among the saline-treated model, MSCs, and Gel groups. In the saline-treated model group, clinical signs of arthritis

began to appear on Day 22 after the first immunization. Treatment with encapsulated MSCs not only delayed the onset of arthritic changes but also significantly reduced the incidence of arthritis (Fig. 4C), articular scores of the ankle joint (Fig. 4D), and hind paw thickness (Fig. 4E), compared to the saline-treated model group, demonstrating the superiority of encapsulated MSCs in alginate hydrogel. The spleen index in the saline-treated model group was increased significantly compared with the control group. In contrast, after the treatment with encapsulated MSCs in alginate hydrogel, the spleen index was decreased significantly (Supporting Information Fig. S4A). The level of adenosine in the serum of CIA mice was analyzed using a mouse adenosine ELISA kit. Compared to the saline-treated model, MSCs, and Gel groups, adenosine concentration in serum was enhanced in encapsulated MSCs group (Fig. S4B). Furthermore, the level of total IgG in saline-treated model group was significantly enhanced, while that in encapsulated MSCs group was significantly decreased compared to the saline-treated model, MSCs, and Gel groups (Fig. S4C). We then measured the levels of pro-inflammatory cytokines and anti-inflammatory cytokines as the index to evaluate the prophylactic efficacy. For the saline-treated mice, the cytokines, including IL-6 and TNF-α, remained at high levels (Fig. S4D and S4E), while the encapsulated MSCs group could reduce these cytokines almost to normal. The level of IL-10 was significantly increased in the encapsulated MSCs group, demonstrating a notable anti-inflammatory and immunosuppressive activity (Fig. S4F). The pro-inflammatory cytokine levels were also significantly decreased with Gel or MSCs treatment, while the prophylactic efficacy against arthritis was much lower in MSCs + Gel treatment group. As expected, the encapsulated MSCs displayed the most obvious preventive effect on CIA, which was contributed by the best immunosuppressive and anti-inflammatory efficacy.

The representative images of the ankle joints and feet in each treatment group on Day 42 after CIA induction were shown in Fig. 4F. Furthermore, microcomputed tomography (micro-CT) imaging of joints isolated at the conclusion of the experiment (4 weeks after treatment) showed a marked reduction in the degree of bone erosion in the hind paws and ankle joints of the MSC + Gel group compared to the other treatment groups (Fig. 4G).

Besides the prophylactic CIA model, we also evaluated the therapeutic effect of encapsulated MSCs. Similarly, encapsulated MSCs significantly inhibited the development of CIA and alleviated the clinical score compared with the model group (Supporting Information Fig. S5). Collectively, all these *in vivo* results suggest superior prophylactic and therapeutic effect of encapsulated MSCs, which is significantly better than that of the treatment of Gel or MSCs alone.

3.5. Encapsulated MSCs suppress autoimmune responses in CIA mice by promoting differentiation of tolDCs and Tregs

Histopathological examination of the arthritic tissues by H&E (Fig. 5A) and Safranin O (Fig. 5B) staining showed there were no

---

MSCs group, (6) is the mice in DiR-labeled MSCs imbedded in alginate hydrogel group. (B) Quantification of the fluorescent signal at different time points post-injection of DiR-labeled MSCs. (C) Ki67 immunostaining of MSCs encapsulated in alginate hydrogel 7 days after s.c. implantation in mice. (D) The count of Ki67^{+} cells in each treatment group. Photograph (E) and H&E staining (F) of MSCs were encapsulated in alginate hydrogel 7 days after s.c. implantation in mice. Expression of CD86^{+} cells (G), proportion of CD86^{+} cells (H), expression of MHCII^{+} cells (I), proportion of MHCII^{+} cells (J), expression of CD73^{+} cells (K), proportion of CD73^{+} cells (L) in inguinal lymph node (LN) analyzed by flow cytometry at day 7 post immunization. Blue lines represent the histogram of negative cells, and red lines represent the histogram of positive cells (G, I and K). Data are represented as mean ± SEM, $n = 3$; **$P < 0.01$, ***$P < 0.001$ *vs.* indicated.
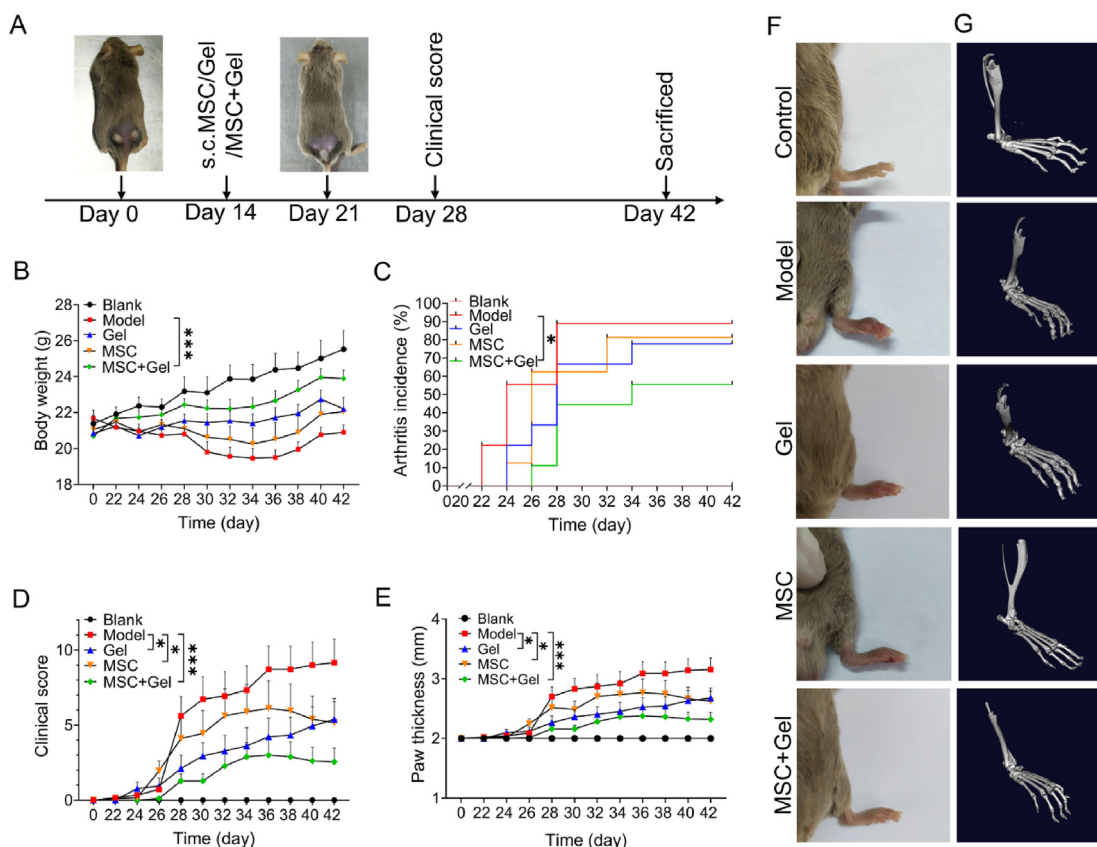
Figure 4 Encapsulated MSCs in alginate hydrogel inhibit arthritis development in prophylactic CIA mice. (A) Schematic representation of the treatment protocol in CIA mice. (B) Body weight of CIA mice after treatment with alginate hydrogel (100 μL), MSCs (1×10^6), the MSCs encapsulated in alginate hydrogel (1×10^6 cells in 100 μL hydrogel). (C) Arthritis incidence of CIA. (D) Clinical score of CIA mice in each treatment group. (E) Paw thickness of CIA mice in each treatment group. (F) Representative photographs of ankle joints and feet after CIA induction for 42 day in each treatment group ($n = 9$ per group). (G) Representative micro-CT images of mouse ankle joints in CIA mice treated with vehicle, alginate hydrogel, MSC alone or with alginate hydrogel on Day 42. Micro-CT images of mouse ankle joints of non-immunized mice were used as controls. Data are represented as mean ± SEM, $n = 6$, $*P < 0.05$, $***P < 0.001$, significantly different from the CIA model group.

obvious synovial hyperplasia, lymphocyte infiltration, cartilage damage, and bone erosion in the affected joints in encapsulated MSCs group (Fig. 5A−C). While mice treated with alginate hydrogel alone still had synovial inflammation, along with cartilage and bone destruction in ankle joints. For the bare MSCs group, the characteristic signs of inflammation, lymphocyte infiltration, and bone erosion were reduced. These results indicated that encapsulation of MSCs in alginate hydrogel strengthened the immunosuppressive ability of MSCs and effectively inhibited arthritic progression and inflammation.

DCs play a crucial role in initiating and augmenting of immune responses during RA progression by presenting self-antigens to T cells and releasing pro-inflammatory cytokines[33]. To further elaborate the effect of encapsulated MSCs on DCs in disease conditions, we evaluated the effect of the encapsulated MSCs on DCs maturation and T cells differentiation in the CIA model to fully elucidate the immunosuppression mechanism of encapsulated MSCs. Briefly, cells isolated from the draining lymph nodes were stained for surface markers of mature DCs and intracellular markers of Treg cells (Fig. 5D−M). Compared to the saline-treated model group, the percentage of CD11c$^+$ cells in mice treated with the encapsulated MSCs was significantly decreased

($P < 0.01$). Interestingly, in the alginate hydrogel group, the percentage of CD11c$^+$ cells was also reduced ($P < 0.05$), albeit to a lesser extent (Fig. 5D and E). There was also a decrease in CD86$^+$ cells ($P < 0.01$) (Fig. 5F and G) and MHCII$^+$ cells ($P < 0.05$) (Fig. 5H and I) in encapsulated MSCs group compared to the saline-treated model group. Furthermore, the percentage of immunotolerant CD73$^+$ DCs and CD73$^+$CD11c$^+$ DCs was increased significantly in mice treated with encapsulated MSCs compared to the saline-treated model group (Fig. 5J and K, Fig. S4G and S4H). There were no significant differences in CD39$^+$ cells in encapsulated MSCs group compared to the saline-treatment group (Fig. S4I and S4J). Finally, we identified the proportion of CD4$^+$ T cells gating from the total lymphocyte population, and in the CD4$^+$ T cells gate, we further analyzed the expression of CD25$^+$ and FoxP3$^+$ cells. It was found that the proportion of CD4$^+$CD25$^+$FoxP3$^+$ Treg cells was considerably enhanced in the lymph nodes of mice treated with the hydrogel-encapsulated MSCs ($P < 0.001$ *vs.* the treatment of saline, Gel, and MSCs; Fig. 5L and M). These results confirmed that encapsulated MSCs could augment immunosuppressive effects by driving tolDCs and Tregs through CD39/CD73 axis, thereby relieving the symptoms of arthritis in mice.
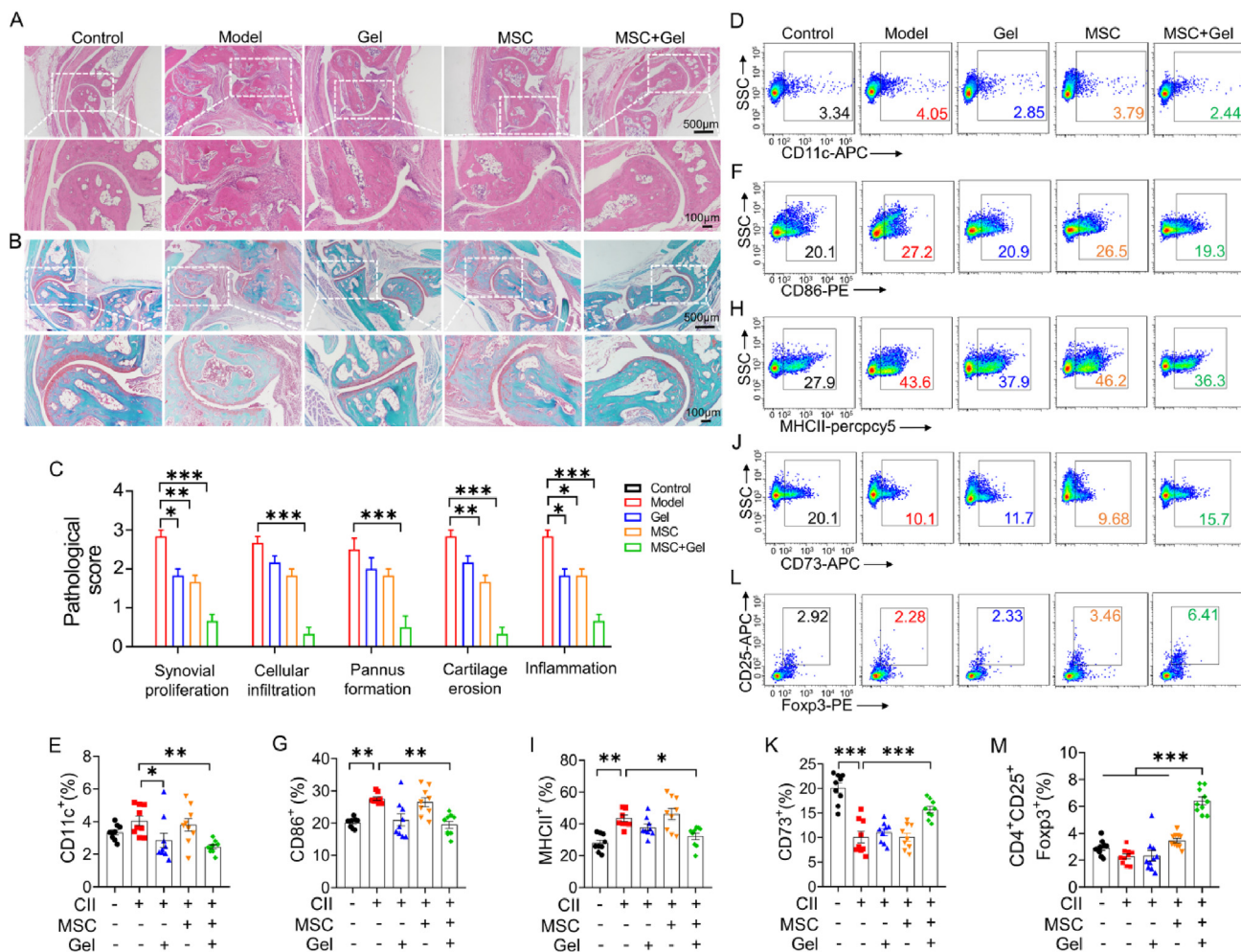
Figure 5 Encapsulated MSCs ameliorate pathological damage in CIA by promoting tolerance of DCs and Treg differentiation. H&E (A) and Safranin O (B) staining of tissue sections (5 μm) of ankle joints of DBA/1 mice on Day 42. Scale bar = 100 μm. (C) Histopathological evaluation of the ankle joint for synovial proliferation, cellular infiltration, pannus formation, cartilage erosion and inflammation ($n = 3$). Expression of CD11c$^+$ cells (D), CD86+ cells (F), MHCII$^+$ cells (H), and CD73$^+$ cells (J), in inguinal LNs from DBA/1 mice on Day 42 were determined by flow cytometry. The proportion of CD11c$^+$ cells (E), CD86$^+$ cells (G), MHCII$^+$ cells (I), and CD73$^+$ cells (K) in inguinal LNs. (L) Flow cytometry analysis of inguinal LN cells by CD4, CD25 and Foxp3 staining. Each plot shows data for an individual mouse ($n = 9$). (M) The proportion of CD4$^+$CD25$^+$Foxp3$^+$ cells in inguinal LNs. Data are represented as mean ± SEM, $n = 9$, *$P < 0.05$, **$P < 0.01$, ***$P < 0.001$, significantly different from the CIA model group.

3.6. Encapsulated MSCs promote tolerogenic differentiation of DCs by activating the adenosine A$_{2A/2B}$ receptor pathway

To further explore the mechanism underlying the immunosuppressive effects of MSCs on DCs in response to an inflammatory stimulus, we co-cultured LPS-stimulated DCs with the bare or encapsulated MSCs and measured the expression levels of various immunoregulatory molecules. We first examined the adenosine levels in the cell's supernatant of different groups. Compared to the control, MSCs treatment group, encapsulated MSCs showed increased release of adenosine in the supernatant, pre-treatment of the co-cultured DCs with the selective antagonist of A$_{2B}$R (LAS01057, 5 μmol/L) and A$_{2A}$R (SCH58261, 5 μmol/L) significantly reversed the effect of the encapsulated MSCs on adenosine (Fig. 6A). Compared to MSCs alone, MSCs in the hydrogel scaffold upregulated the protein expression of the adenosine receptors (ARs) A$_{2A}$R (Fig. 6E and F) and A$_{2B}$R (Fig. 6E and G), indoleamine 2,3-dioxygenase (IDO) (Fig. 6E and

H) and programmed cell death ligand-1 (PDL-1) (Fig. 6B and D), which are known immunosuppressive factors targeting DCs. Furthermore, pre-treatment of the co-cultured DCs with the selective antagonist of A$_{2B}$R and A$_{2A}$R significantly reversed the immunosuppressive effects of the encapsulated MSCs. Meanwhile, we also measured the mRNA expression of various immunoregulatory molecules. Compared to MSCs alone, MSCs in the hydrogel scaffold upregulated the transcripts of the adenosine receptors (ARs) A$_{2A}$R and A$_{2B}$R, indoleamine 2,3-dioxygenase (IDO) and programmed cell death ligand-1 (PDL-1) (Supporting Information Fig. S6A, S6C, S6E, and S6G). Furthermore, pre-treatment of the co-cultured DCs with the selective antagonist of A$_{2B}$R and A$_{2A}$R significantly reversed the immunosuppressive effects of the encapsulated MSCs (Figs. S6A, S6C, S6E, and S6G). However, they had little effect on MSCs alone (Figs. S6B, S6D, S6F, and S6H). Given that these receptors are G-coupled, we measured the activity of A$_{2A}$R and A$_{2B}$R based on intracellular cyclic (cAMP) accumulation. As shown in
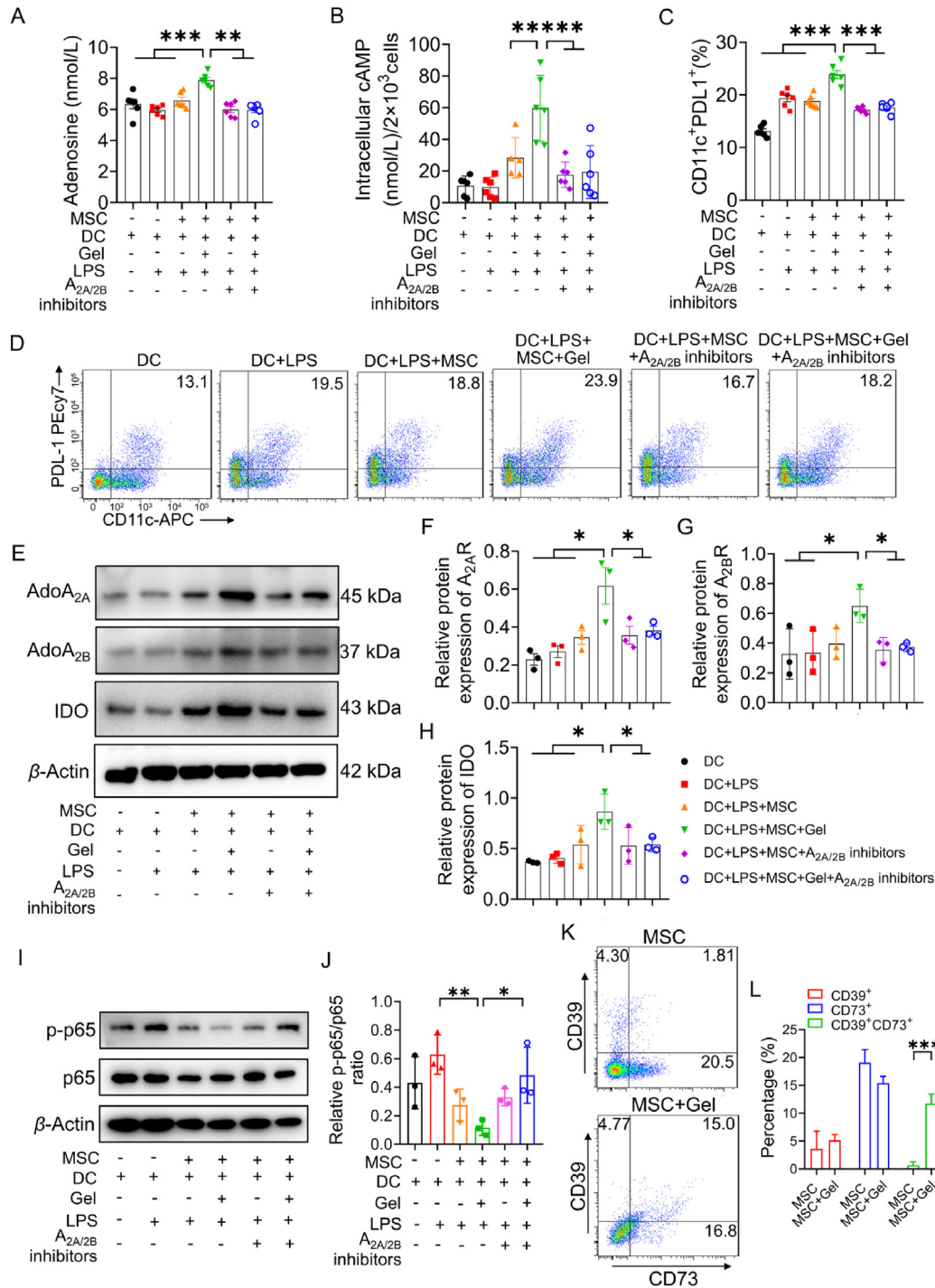
Figure 6 Encapsulated MSCs impair BMDC maturation through activating $A_{2A/2B}AR$. (A) Concentration of adenosine in supernatant of BMDCs stimulated with 100 ng/mL LPS and exposed to encapsulated MSCs. (B) BMDCs were stimulated with 100 ng/mL LPS and exposed to encapsulated MSCs in the presence of 0.5 mmol/L IBMX. Accumulation of cAMP was measured by a cAMP Gs Dynamic assay. (C and D) Flow cytometry analysis of $CD11c^+PDL\text{-}1^+$ cells in BMDCs stimulated with 100 ng/mL LPS and exposed to encapsulated MSCs. (E–H) Western blotting was performed to detect the protein expression of $A_{2A}R$, $A_{2B}R$, and IDO (E), relative protein expression of $A_{2A}R$ (F), relative protein expression of $A_{2B}R$ (G), relative protein expression of IDO (H). (I) Western blotting was performed using the cell lysates in RIPA buffer to detect phosphorylated p65 and total p65 levels. (J) Relative p-p65/p65 expression was shown. (K) The expression of CD39 and CD73 on MSCs and encapsulated MSCs was detected using flow cytometry. (L) Representative percentage of $CD39^+$, $CD73^+$, and $CD39^+CD73^+$ was shown. Data are represented as mean $\pm$ SD, $n = 3$, *$P < 0.05$, **$P < 0.01$, ***$P < 0.001$ vs. indicated, ns, not significant.

Fig. 6C, Bone marrow-derived dendritic cells (BMDCs) co-cultured with the encapsulated MSCs in the presence of LPS had significantly elevated cAMP compared to cells treated with alginate hydrogel or without LPS stimulation. The adenosine/cAMP-dependent activation of protein kinase A (PKA) downstream of $A_{2A}R$ and $A_{2B}R$ selectively suppresses the pro-inflammatory NF-κB pathway[34]. Our results also indicated that MSCs encapsulated in alginate hydrogel suppressed LPS-induced activation of the NF-κB pathway (Fig. 6I and J). Adenosine/cAMP is generated following the hydrolysis of extracellular ATP (eATP), a potent stimulatory factor for DCs, by CD39 and CD73[35]. The transmembrane CD39 hydrolyzes eATP into ADP and eAMP, and CD73 converts eAMP to adenosine, which exerts immunosuppressive effects *via* A_{2A} and A_{2B} receptors[36,37]. Our data showed that LPS-stimulation significantly increased the ATP release from DCs, suppressed by the encapsulated MSCs, with simultaneous upregulation of CD39 and CD73 (Fig. 6K and L).

3.7. Adenosine $A_{2A/2B}R$ activation on BMDCs alleviate inflammatory responses by inducing Treg differentiation

Previous studies showed that the expression of inflammation-related factors, such as TNF-α, IL-12p70, and IL-10, are regulated by $A_{2A/2B}$ receptor ($A_{2A/2B}R$) signaling in murine BMDCs[14,38]. LPS stimulation significantly increased the production of pro-inflammatory cytokines, including TNF-α, IL-12p70, and IL-6 in DCs, and downregulated the anti-inflammatory IL-10. These changes were reversed in the presence of the encapsulated MSCs (Fig. 7A–H). Furthermore, the $A_{2A/2B}AR$ antagonists neutralized the effect of the encapsulated MSCs on the cytokine responses of DCs but had minimum impact on the bare MSCs. Compared to the MSCs alone group, adding $A_{2A/2B}R$ antagonists can reverse the effect of MSCs encapsulated in alginate hydrogel on DCs in cytokine responses. Taken together, the immunosuppressive effects of the encapsulated MSCs on DCs were mediated by the activation of $A_{2A}R$ and $A_{2B}R$.

To determine whether DCs activated by the encapsulated MSCs regulate T cell differentiation, DCs subjected to LPS, LPS + MSC, LPS + MSC + $A_{2A/2B}R$ inhibitors, Gel, Gel + LPS, Gel + LPS + MSC, or Gel + LPS + MSC + $A_{2A/2B}R$ inhibitors were co-cultured with lymph node T cells for 5 days (Fig. 7I). T cell differentiation was evaluated by measuring the levels of cytokines characteristic to Th1 (IFN-γ and TNF-α), Th17 (IL-17A), and Treg (IL-10) cells. LPS-stimulated BMDCs co-cultured with the encapsulated MSCs inhibited Th1 and Th17 differentiation and promoted the induction of IL-10-producing Treg cells (Fig. 7J–Q). The inhibitor of $A_{2A/2B}R$ simultaneously reversed the effect of the encapsulated MSCs on T-cell differentiation induced by LPS-stimulated BMDCs. To summarize, MSCs encapsulated in alginate hydrogel can mitigate inflammation by inducing tolDCs and Treg cells by activating the CD39/CD73-mediated $A_{2A/2B}R$ axis.

4. Discussion

Here, we describe for the first time that MSCs encapsulated in alginate hydrogel promote the differentiation of CD73$^+$ tolDCs and Tregs through CD39/CD73-$A_{2A/2B}R$ axis to retard arthritic progression. Our findings are consistent with that reported by Zhang and coworkers[39], wherein MSCs suppressed the development of monocyte derived DCs *in vitro*.

Alginate hydrogel is an ideal scaffold for biomedical applications, given its ability to rapidly form non-covalent crosslinks, controllable mechanical properties, and good biocompatibility. In this study, we crosslinked the hydrogel with Ca^{2+} and found that 5.0% alginate provided adequate mechanical stiffness. The hydrogel scaffold induced the proliferation and 3D spreading of the MSCs *in vitro*, and prolonged the retention of encapsulated MSCs *in vivo*. Subcutaneous transplantation of hydrogel matrix provided an appropriate niche for MSCs to proliferate and recruit inflammatory immune cells to crosstalk, differentiating immature DCs into tolDCs in the draining lymph nodes by decreased expression of CD86, MHCII, and TNF-α, and increased the expression of IDO, PDL1, and IL-10. The *in vivo* immunosuppressive effect of the encapsulated MSCs translated to improved therapeutic outcomes against arthritis.

The complex pathophysiology and microenvironment of RA were simulated by immunizing mice with CII/CFA to evaluate the immunosuppressive function of the encapsulated MSCs. The CIA model can reproduce the major pathological characteristics observed in human RA. Synovial fluid from RA patients contains higher numbers of DCs than the peripheral blood, reflecting the role of antigen-presenting cells in disease progression[40]. The peripheral DCs migrate to synovial fluid, where local factors or cytokines, and present antigens to specific T cells activate them. Synovial DCs isolated from RA patients show upregulation of co-stimulatory molecules, MHC molecules, and RelB. DCs also secrete inflammatory cytokines that promote the differentiation of naïve T cells to Th1 or Th17 subsets[41]. Furthermore, DCs can direct the maturation of antibody-secreting B cells as well[42]. Thus, targeting DC is a pivotal and novel treatment strategy for RA. Interestingly, the recognition and phagocytosis of self-antigens from apoptotic debris transform iDCs to tolDCs, which produce immunosuppressive cytokines and initiate cross-tolerance. TolDCs can still migrate into lymph nodes and present antigens to T cells, resulting in decreased expression of CD86 and CD80 and increased production of immunosuppressive mediators, such as IDO, IL-10, and CD39/CD73. The therapeutic potential of tolDCs has been assessed in animal model[9]. For instance, tolDCs generated by silencing B cell activating factor (BAFF) alleviated the arthritic symptoms and restored the Treg/Th17 balance in CIA mice[7,40]. Besides, DCs can also maintain immunotolerance by inducing Treg cells.

Adenosine signaling is associated with the immunoregulatory function of MSCs and DCs[42,43], and is therefore, a promising therapeutic target for RA. Adenosine is a neurotransmitter that is produced by the degradation of eATP and the concerted action of CD39 and CD73. While eATP acts as a "danger" signal that triggers inflammatory responses, adenosine has an anti-inflammatory function mediated by down-regulation of DCs activity, T cell activation, and cytokines secretion[44]. MSCs release immunosuppressive molecules such as IDO, TGF-β, PGE$_2$, and IL-10[45], and upregulate CD39 and CD73 on DCs. Blocking the adenosine signaling pathway by CD39 inhibitor almost blocked MSC-mediated suppression of T cell proliferation[42]. Our data showed that MSCs encapsulated in alginate hydrogel significantly increased the surface expression of CD39 and CD73 on the co-cultured DCs, which increased the production of adenosine and activated the A_{2A} and $A_{2B}R$ on DCs. Wilson and coworkers[27] reported that the non-selective adenosine receptor (AR) agonist NECA significantly inhibited the costimulatory molecules CD86 and MHCII in LPS-stimulated BMDCs and affected the production of TNF-α and IL-10. Their study suggested that $A_{2B}R$ is the
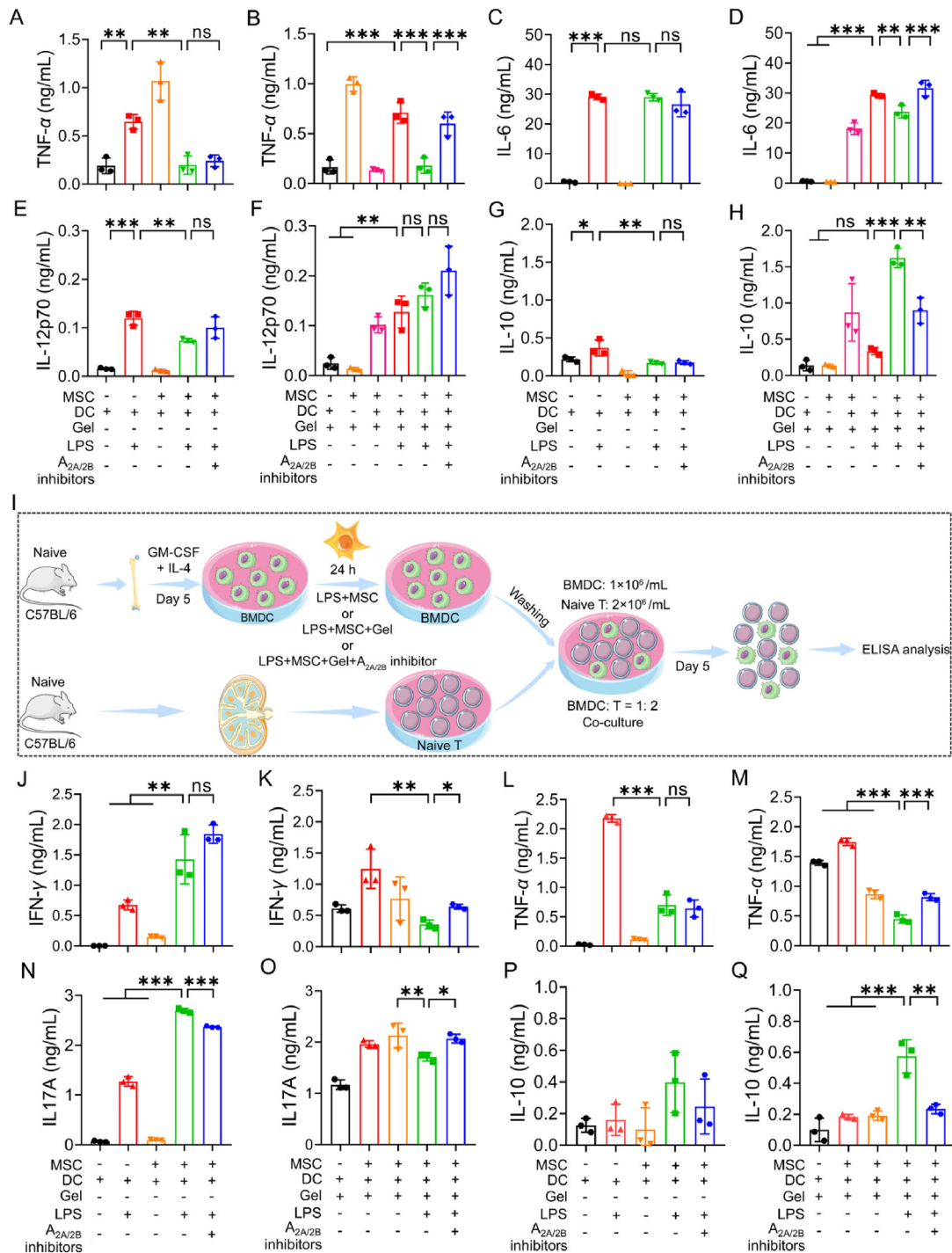
Figure 7 Encapsulated MSCs promote anti-inflammatory tolDCs by inhibiting Th1 and Th17 and inducing differentiation of Treg cells. (A) Inhibition of inflammatory mediator TNF-α in LPS-stimulated BMDCs treated with MSCs. (B) Inhibition of inflammatory mediator TNF-α in LPS-stimulated BMDCs treated with encapsulated MSCs and using $A_{2A/2B}R$ inhibitor can reverse this function. (C) Expression of IL-6 in LPS-stimulated BMDCs treated with MSCs. (D) Inhibition of IL-6 in LPS-stimulated BMDCs treated with encapsulated MSCs and using $A_{2A/2B}R$ inhibitors can reverse this function. (E) Inhibition of IL-12p70 in LPS-stimulated BMDCs treated with MSCs. (F) Expression of IL-12p70 in LPS-stimulated BMDCs treated with encapsulated MSCs and using $A_{2A/2B}R$ inhibitor can reverse this function. (G) Promotion of anti-inflammatory mediator IL-10 in LPS-stimulated BMDCs treated with MSCs. (H) Promotion of anti-inflammatory mediator IL-10 in LPS-stimulated BMDCs treated with encapsulated MSCs and using $A_{2A/2B}R$ inhibitor can reverse this function. TNF-α, IL-6, IL-12p70, and IL-10 were measured by ELISA. (I) Graphical representation of the experimental strategy for BMDCs and T cells co-culture system. (J and K) Supernatants of IFN-γ from the T cells co-culture system were performed after 5 days to test Th1 cells differentiation. (L and M) Supernatants of TNF-α from T cells co-culture system were performed after 5 days to assess Th1 cell differentiation. (N and O) Supernatants of IL-17A from the T cells co-culture system were performed after 5 days to evaluate Th17 cells differentiation. (P and Q) Supernatants of IL-10 from T cells co-culture system were performed after 5 days to evaluate Treg cells differentiation. Data are represented as mean ± SD, $n = 3$, $*P < 0.05$, $**P < 0.01$, $***P < 0.001$ vs. indicated, ns, not significant.
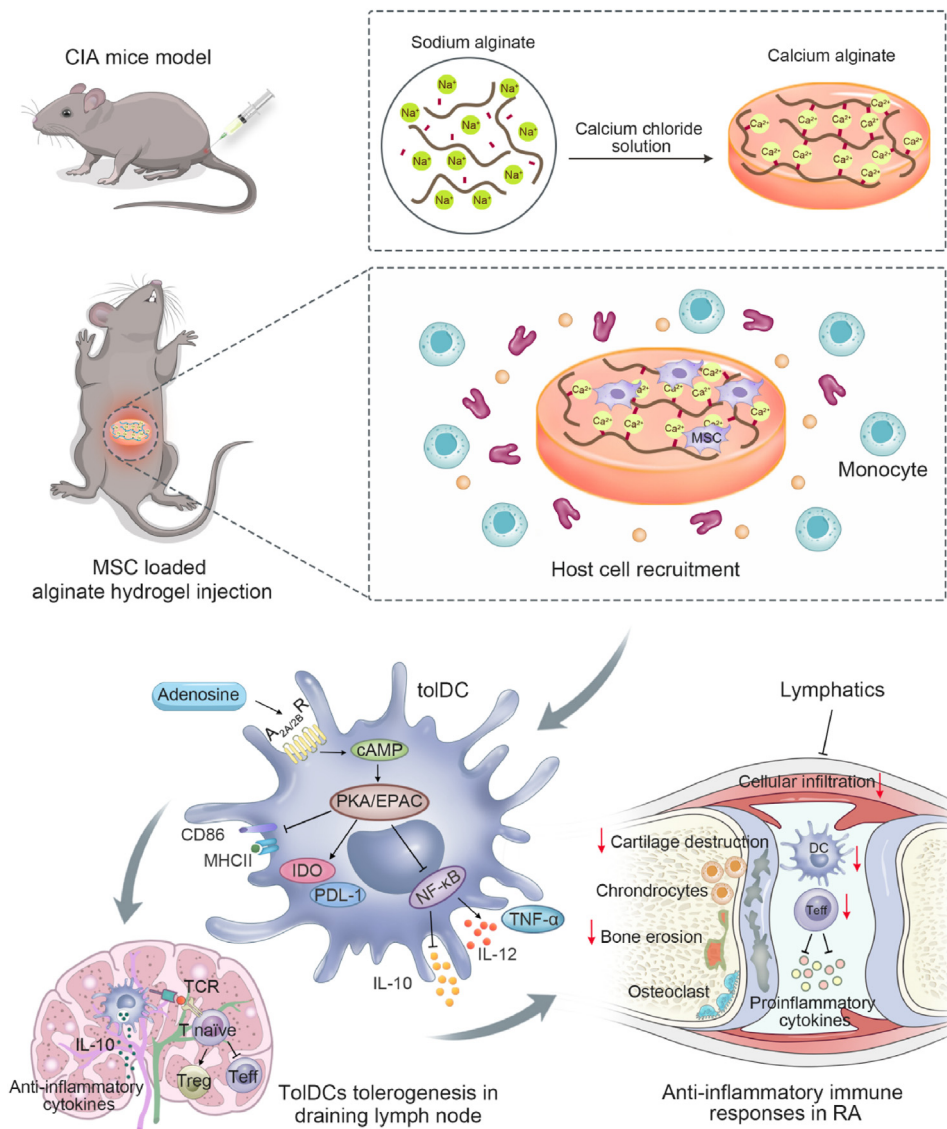
Figure 8   A schematic illustration of encapsulated MSCs and their proposed mechanism. Encapsulated MSCs in alginate hydrogel ameliorate arthritis inflammation by activating adenosine $A_{2A/2B}$ receptor to induce the transformation of immature DCs to tolDCs and further regulate naïve T cells into Tregs.

predominant immunoregulatory receptor in BMDCs. Two more recent studies have also demonstrated that $A_{2B}R$ modulated DC development and function[46]. Consistent with previous reports, we found that the encapsulated MSCs activated $A_{2A/2B}R$ downregulated the expression of CD86 on the LPS-stimulated DCs, and inhibited the production of TNF-α, all of which were descriptive of a tolerogenic phenotype[47]. Besides, pre-treatment with $A_{2A/2B}R$ inhibitors reversed the induction of tolDCs by the encapsulated MSCs. These findings indicated that the immunosuppressive effect of the encapsulated MSCs was *via* the activation of $A_{2A/2B}$ receptors mediated by CD39/CD73. The $A_{2A/2B}R$ signaling pathway elevates cytoplasmic cAMP, a strong immunosuppressive factor. The increased cAMP levels in DCs can retard inflammation through adenosine/cAMP-mediated blockade of NF-κB activity[34]. Interestingly, the $A_{2A/2B}R$ inhibitors rescued adenosine-mediated inactivation of NF-κB in the DCs co-cultured with the encapsulated MSCs but not the bare MSCs. This strongly suggested that

the CD39/CD73/adenosine-mediated immunosuppressive effect on DCs occurs through the negative regulation of the NF-κB signaling pathway. Future studies will focus on characterizing the therapeutic potential of targeting $A_{2A}R$ activation on DCs in autoimmune diseases. To summarize our findings, alginate hydrogel is a suitable matrix for the proliferation, retention, and immunosuppressive function of MSCs, and it should be investigated further as treatment strategies for immune-associated diseases.

5.   Conclusions

An injectable alginate hydrogel as a safe and effective platform was used to deliver MSCs for treating CIA and provided a suitable microenvironment for immature DCs infiltrating the scaffold from the draining lymph nodes and interacted with MSCs. Furthermore,

transplantation of the encapsulated MSCs achieved long-term proliferation and engraftment in CIA mice and mitigated inflammatory tissue damage by creating an immunosuppressive microenvironment to promote $A_{2A/2B}R$-mediated differentiation of tolDCs and Treg cells (Fig. 8). In summary, local injection of alginate hydrogel encapsulated MSCs is a promising therapeutic strategy against inflammatory and autoimmune disorders.

Acknowledgments

Author contributions

Gaona Shi, Weiwei Wang, Lan Sun, and Tiantai Zhang designed the study. Gaona Shi, Yu Zhou, Wenshuai Liu, Chengjuan Chen and Yazi Wei performed the experiments, analyzed the data, and prepared the figures and tables. Gaona Shi, Yu Zhou, and Chengjuan Chen contributed to the animal studies. Gaona Shi, Weiwei Wang, Lan Sun, and Tiantai Zhang wrote the paper. Xinlong Yan and Lei Wu provided critical input and edited the draft. Weiwei Wang, Lan Sun and Tiantai Zhang performed supervision, project administration, and funding acquisition. Tiantai Zhang supervised and coordinated all the work. All authors read and approved the final manuscript.

Conflicts of interest

The authors declare no conflicts of interest.

Appendix A. Supporting information

Supporting data to this article can be found online at https://doi.org/10.1016/j.apsb.2023.04.003.

References

1. Klareskog L, Catrina AI, Paget S. Rheumatology arthritis. *Lancet* 2009;**373**:659−72.
2. Schett G, Gravallese E. Bone erosion in rheumatoid arthritis: mechanisms, diagnosis and treatment. *Nat Rev Rheumatol* 2012;**8**:656−64.
3. McInnes IB, Schett G. The pathogenesis of rheumatoid arthritis. *N Engl J Med* 2001;**365**:2205−19.
4. Liu Y, Rao PS, Qian HY, Shi YS, Chen SJ, Lan JY, et al. Regulatory fibroblast-like synoviocytes cell membrane coated nanoparticles: a novel targeted therapy for rheumatoid arthritis. *Adv Sci* 2022;**9**: e2204998.
5. Hoes JN, Jacobs JW, Buttgereit F, Bijlsma JW. Current view of glucocorticoid co-therapy with DMARDs in rheumatoid arthritis. *Nat Rev Rheumatol* 2010;**6**:693−702.
6. Yang YH, Guo LN, Wang Z, Liu P, Liu XJ, Ding JS, et al. Targeted silver nanoparticles for rheumatoid arthritis therapy *via* macrophage apoptosis and Re-polarization. *Biomaterials* 2021;**264**: 120390.
7. Zhao YJ, Sun XJ, Yang XZ, Zhang BJ, Li SY, Han P, et al. Tolerogenic dendritic cells generated by BAFF silencing ameliorate collagen-induced arthritis by modulating the Th17/regulatory T cell balance. *J Immunol* 2020;**204**:518−30.
8. Nygaard G, Firestein GS. Restoring synovial homeostasis in rheumatoid arthritis by targeting fibroblast-like synoviocytes. *Nat Rav Rheumatol* 2020;**16**:316−33.
9. Choy EH, Kavanaugh AF, Jones SA. The problem of choice: current biologic agents and future prospects in RA. *Nat Rev Rheumatol* 2013; **9**:154−63.
10. Ankrum JA, Ong JF, Karp JM. Mesenchymal stem cells: immune evasive, not immune privileged. *Nat Biotechnol* 2014;**32**:25262.
11. Ansboro S, Roelofs AJ, De Bari C. Mesenchymal stem cells for the management of rheumatoid arthritis: immune modulation, repair or both? *Curr Opin Rheumatol* 2017;**29**:201−7.
12. Papadopoulou A, Yiangou M, Athanasiou E, Zogas N, Kaloyannidis P, Batsis I, et al. Mesenchymal stem cells are conditionally therapeutic in preclinical models of rheumatoid arthritis. *Ann Rheum Dis* 2012;**71**: 1733−40.
13. Ranganath SH, Levy O, Inamdar MS, Karp JM. Harnessing the mesenchymal stem cell secretome for the treatment of cardiovascular disease. *Cell Stem Cell* 2012;**10**:244−58.
14. Nicola MD, Carlo-Stella C, Magni M, Milanesi M, Longoni PD, Matteucci P, et al. Human bone marrow stromal cells suppress T-lymphocyte proliferation induced by cellular or nonspecific mitogenic stimuli. *Blood* 2002;**99**:3838−43.
15. Bartosh TJ, Ylöstalo JH, Mohammadipoor A, Bazhanov N, Coble K, Claypool K, et al. Aggregation of human mesenchymal stromal cells (MSCs) into 3D spheroids enhances their antiinflammatory properties. *Pro Natl Acad Sci USA* 2010;**107**:13724−9.
16. Kwon SG, Kwon YW, Lee TW, Park GT, Kim JH. Recent advances in stem cell therapeutics and tissue engineering strategies. *Biomater Res* 2018;**22**:36.
17. Turnbull G, Clarke J, Picard F, Riches P, Jia LL, Han FX, et al. 3D bioactive composite scaffolds for bone tissue engineering. *Bioact Mater* 2018;**3**:278−314.
18. Hernández-González AC, Téllez-Jurado L, Rodríguez-Lorenzo LM. Alginate hydrogels for bone tissue engineering, from injectables to bioprinting: a review. *Carbohydr Polym* 2020;**229**:115514.
19. Yang PX, Song HJ, Qin YB, Huang PS, Zhang CN, Kong DL, et al. Engineering dendritic-cell-based vaccines and PD-1 blockade in self-assembled peptide nanofibrous hydrogel to amplify antitumor T-cell immunity. *Nano Lett* 2018;**18**:4377−85.
20. Zhu H, Guo ZK, Jiang XX, Li H, Wang XY, Yao HY, et al. A protocol for isolation and culture of mesenchymal stem cells from mouse compact bone. *Nat Protoc* 2010;**5**:550−60.
21. Shi GN, Zhang CN, Xu R, Niu JF, Song HJ, Zhang XY, et al. Enhanced antitumor immunity by targeting dendritic cells with tumor cell lysate-loaded chitosan nanoparticles vaccine. *Biomaterials* 2017; **113**:191.
22. Shi GN, Hu M, Chen C, Fu J, Shao S, Zhou Y, et al. Methotrexate enhances antigen presentation and maturation of tumour antigen-loaded dendritic cells through NLRP3 inflammasome activation: a strategy for dendritic cell-based cancer vaccine. *Ther Adv Med Oncol* 2021;**13**:1758835920987056.
23. Chen CJ, Yin Y, Shi GN, Zhou Y, Shao S, Wei YZ, et al. A highly selective JAK3 inhibitor is developed for treating rheumatoid arthritis

by suppressing γc cytokines related JAK-STAT signal. *Sci Adv* 2022;**8**:eabo4363.

24. Bai M, Zhang L, Fu B, Bai JX, Zhang YJ, Cai GY, et al. IL-17A improves the efficacy of mesenchymal stem cells in ischemic-reperfusion renal injury by increasing Treg percentages by the COX-2/PGE2 pathway. *Kidney Int* 2018;**93**:814−25.

25. Han CC, Li YF, Zhang YW, Wang Y, Cui DQ, Luo TT, et al. Targeted inhibition of GRK2 kinase domain by CP-25 reverse fibroblast-like synoviocytes dysfunction and improve collagen-induced arthritis in rats. *Acta Pharm Sin B* 2021;**11**:1835−52.

26. Xin WY, Huang C, Zhang X, Xin S, Zhou YM, Ma XW, et al. Methyl salicylate lactoside inhibits inflammatory response and joint destruction on fibroblast-like synoviocytes and collagen-induced arthritis mice. *Br J Pharmacol* 2014;**171**:3526−38.

27. Lappas CM, Rieger JM, Linden J. A2A adenosine receptor induction inhibits IFN-γ production in murine CD4⁺ T cells. *J Immunol* 2005;**174**:1073−80.

28. Hao T, Li JJ, Yao FL, Dong DY, Wang Y, Yang BG, et al. Injectable fullerenol/alginate hydrogel for suppression of oxidative stress damage in brown adipose-derived stem cells and cardiac repair. *ACS Nano* 2017;**11**:5474−88.

29. Monteiro CF, Santos SC, Custódio CA, Mano JF. Human platelet lysates-based hydrogels: a novel personalized 3D platform for spheroid invasion assessment. *Adv Sci* 2020;**7**:1902398.

30. Le Blanc K, Mougiakakos D. Multipotent mesenchymal stromal cells and the innate immune system. *Nat Rev Immunol* 2012;**12**:38396.

31. Hawrylowicz CM, O'Garra A. Potential role of interleukin-10-secreting regulatory T cells in allergy and asthma. *Nat Rev Immunol* 2005;**5**:271−83.

32. O'Garra A, Barrat FJ, Castro AG, Vicari A, Hawrylowicz C. Strategies for use of IL-10 or its antagonists in human disease. *Immunol Rev* 2008;**223**:114−31.

33. Ji H, Ohmura K, Mahmood U, Lee DM, Hofhuis FMA, Boackle SA, et al. Arthritis critically dependent on innate immune system players. *Immunity* 2002;**16**:157−68.

34. Minguet S, Huber M, Rosenkranz L, Schamel WW, Reth M, Brummer T. Adenosine and cAMP are potent inhibitors of the NF-*k*B pathway downstream of immunoreceptors. *Eur J Immunol* 2005;**35**:31−41.

35. Kaczmarek E, Koziak K, Sévigny J, Siegel JB, Anrather J, Beaudoin AR, et al. Identification and characterization of CD39/vascular ATP diphosphohydrolase. *J Biol Chem* 1996;**271**:33116−22.

36. Zimmermann H. 5'-Nucleotidase: molecular structure and functional aspects. *Biochem J* 1992;**285**:345−65.

37. Cekic C, Linden J. Purinergic regulation of the immune system. *Nat Rev Immunol* 2016;**16**:177−92.

38. Panther E, Corinti S, Idzko M, Herouy Y, Napp M, la Sala A, et al. Adenosine affects expression of membrane molecules, cytokine and chemokine release, and the T-cell stimulatory capacity of human dendritic cells. *Blood* 2003;**101**:3985−90.

39. Zhang W, Ge W, Li CH, You SG, Liao LM, Han Q, et al. Effects of mesenchymal stem cells on differentiation, maturation, and function of human monocyte-derived dendritic cells. *Stem Cells Dev* 2004;**13**:263−71.

40. Khan S, Greenberg JD, Bhardwaj N. Dendritic cells as targets for therapy in rheumatoid arthritis. *Nat Rev Rheumatol* 2009;**5**:566−71.

41. Zhou L, Chong MMW, Littman DR. Plasticity of CD4⁺ T cell lineage differentiation. *Immunity* 2009;**30**:646−55.

42. Luo Y, Wu WB, Gu J, Zhang XM, Dang JL, Wang JL, et al. Human gingival tissue-derived MSC suppress osteoclastogenesis and bone erosion *via* CD39-adenosine signal pathway in autoimmune arthritis. *EBioMedicine* 2019;**43**:620−31.

43. Kayhan M, Koyas A, Akdemir I, Savas AC, Cekic C. Adenosine receptor signaling targets both PKA and Epac pathways to polarize dendritic cells to a suppressive phenotype. *J Immunol* 2019;**203**:3247−55.

44. Silva-Vilches C, Ring S, Mahnke K. ATP and its metabolite adenosine as regulators of dendritic cell activity. *Front Immunol* 2018;**9**:2581.

45. Zhang QZ, Shi SH, Liu Y, Uyanne J, Shi YF, Shi ST, et al. Mesenchymal stem cells derived from human gingiva are capable of immunomodulatory functions and ameliorate inflammation-related tissue destruction in experimental colitis. *J Immunol* 2009;**183**:7787−98.

46. Ben Addi A, Lefort A, Hua X, Libert F, Communi D, Ledent C, et al. Modulation of murine dendritic cell function by adenine nucleotides and adenosine: involvement of the A(2B) receptor. *Eur J Immunol* 2008;**38**:1610−20.

47. Rutella S, Danese S, Leone G. Tolerogenic dendritic cells: cytokine modulation comes of age. *Blood* 2006;**108**:1435.